VERTICAL TEST RESULTS ON THE STF BASELINE 9-CELL CAVITIES AT KEK

E. Kako#, H. Hayano, S. Noguchi, T. Shishido, K. Umemori, K. Watanabe, Y. Yamamoto,
KEK, Tsukuba, 305-0801, Japan,
H. Sakai, K. Shinoe, ISSP, Univ. of Tokyo, Kashiwa, 277-8581, Japan
S.I. Moon, POSTECH, Pohang, 790-784, Korea, Q.J. Xu, IHEP, Beijing, 100049, China

Abstract

The STF-Baseline superconducting cavity system, which includes four TESLA-type 9-cell cavities, input couplers and frequency tuners, has been developed for the future ILC project. A main improvement in the cavity system is a very stiff design in a He vessel and a cavity tuning system, which can relax a cavity deformation due to Lorentz force. Making clear the performance level of four 9-cell cavities, which were fabricated by a Japanese company and were prepared by existent infrastructures at KEK, is the most important purpose in the whole vertical test. Total 14 vertical tests on four 9-cell cavities were carried out repeatedly. The obtained Eacc,max in the final performance was 29.4 MV/m in the #2 cavity, and the others are 20.8, 20.5 and 20.2 MV/m, where the Qo values higher than $1x10^{10}$ was achieved in all cavities. Peculiar phenomena, like increasing of Qo values with higher Eacc or very slow degradation of Qo values, were observed in the vertical tests. Summary of the vertical test results on four 9-cell cavities is described in this paper.

INTRODUCTION

Construction of STF (Superconducting RF Test Facility) is being carried out at KEK, [1]. The main purpose of STF is to develop the cryomodule including high performance cavities and to establish the industrial design of a Main-Linac unit for ILC (International Linear Collider). One of the important tasks is to carry out high power tests of the STF cryomodule, which includes four TESLA-type STF-Baseline 9-cell cavities and four Low-Loss-type High-Gradient 9-cell cavities. Stable pulsed operation with beam and reliability as a total system with superconducting cavities will be confirmed in the STF Phase-1. Presently, assembly of a 6m-cryomodule including one of four STF-Baseline cavities had completed for the initial test, called the STF Phase-0.5. The first cool-down test of the cryomodule had been started in October, 2007. Design, fabrication and component tests of the STF-Baseline cavity system have been reported in the references, [2, 3]. In this paper, the summary of the vertical tests on four 9-cell cavities and the present status of the STF cryomodule are presented.

STF BASELINE 9-CELL CAVITIES

A superconducting cavity system consists of a 9-cell niobium cavity with thick titanium endplates, an input coupler with cold and warm rf windows [4], two types of HOM couplers [5], a mechanical tuner with a stepping motor and a piezo element [6], a titanium He vessel and a magnetic shield inserted in the He vessel. The specific feature of the STF-Baseline cavity, as shown in Fig. 1, is an improved stiffness of the total cavity supporting system consisting of endplates, a cylinder and a tuning mechanism. Comparison with the TESLA cavity is shown in Table 1. Added modifications are summarised as follows:

- Improved support stiffness by thick titanium endplates.
- Enlarged diameter of beam pipes to compensate a weakened input coupling due to a thick endplate.
- Enlarged diameter of an input port to make an usable rf window larger to raise up a power capability.
- Re-optimisation of cell shape to decrease a ratio of a surface peak magnetic field and an accelerating field.
- Over-coupling of an input coupler for making a band width widen to assure more stable operation.

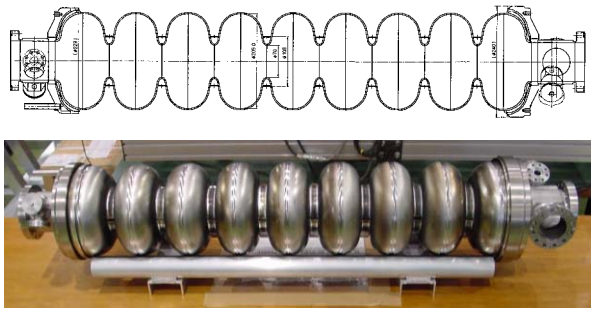

Figure 1: The STF Baseline 9-cell Cavity.

Table 1: Comparison of the main cavity parameters.

Cavity	TESLA	STF-Baseline
Cell Taper	76.7 °	80. °
Φ Beam pipe	78 mm	84 mm
Φ Input port	40 mm	60 mm
Esp / Eacc	1.98	2.17
Hsp / Eacc	42.6 Oe/MV/m	41.0 Oe/MV/m
R / Q	1036 Ω	1016 Ω
Input Coupling	3.0×10^6	2.0×10^6
Support Stiffness	22 kN/mm	72 kN/mm
Lorentz Detuning at 31.5 MV/m	- 500 Hz in a flat top	- 150 Hz in a flat top

#eiji.kako@kek.jp

As a result of the improved cavity supporting system, the stiffness has increased from 22 to 72 kN/mm. Therefore, suppression of the Lorentz-force detuning from -500 to -150 Hz (in a flat top) is expected in a pulsed operation at 31.5 MV/m. Confirmation of this improved effect is the most interesting experiment in high power tests of the cryomodule.

CAVITY PERFORMANCES

Making clear the performance level of four 9-cell cavities, which were fabricated by "a Japanese company, MHI" [7] and were prepared by "existent infrastructures at KEK", is the most important purpose in the whole vertical test.

Surface Preparation

After the initial rf measurements and the dimension check, the 1st step of the standard surface treatments is

- Barrel polishing of about 100 μm.
- Initial electro-polishing (EP-I) of 100 μm.
- Annealing for hydrogen degassing at 750 °C for 3 h.

Pre-tuning for adjusting the frequency (1297.4 MHz) and the field flatness (>97%) was performed. After that, a procedure for the final surface treatments is

- Final electro-polishing (EP-II) of 50 μm.
- Hot water rinsing with ultrasonic bath at 50 °C for 1h.
- High pressure rinsing (HPR) with 8 MPa for 6 ~16 h.
- Baking at 120 °C for 40 h.
- (Optionally, HF or H_2O_2 rinsing for 1 h after EP-II).

Additional EP-II of 20~30 μm was repeated in the successive tests. After one series of initial vertical tests, the 2nd barrel polishing was carried out to increase the surface removal, especially at the equator EBW seam. The average total surface removal came finally to about 500 μm in all cavities.

Vertical Test Results

Not only Qo-Eacc curve and x-ray radiation level, but also Eacc,max in each cell determined by passband mode measurements and search for a heating cell due to quench detected by thermometry, are important to understand the cavity performance in detail. Total 14 vertical tests on four 9-cell cavities were carried out for one year, and the results are summarised in Fig. 2. Rinsing with H_2O_2 after the final EP was applied in the last two tests, and notable decrease of the x-ray radiation level was observed in these tests, although only two cases. The obtained maximum accelerating gradient (Eacc,max) in each cavity and the distribution are shown in Fig. 3 and Fig. 4. The average Eacc,max is 20.3 MV/m, and the limitation was due to quench in all tests, except one case (heating at HOM antenna ; see the next section). The final performances of four 9-cell cavities are shown in Fig. 5. The obtained Eacc,max was 29.4 MV/m in the #2 cavity, and the others are 20.8, 20.5 and 20.2 MV/m, where no steep Qo drop due to field emission was observed, and the Qo values higher than $1x10^{10}$ was obtained in all cavities.

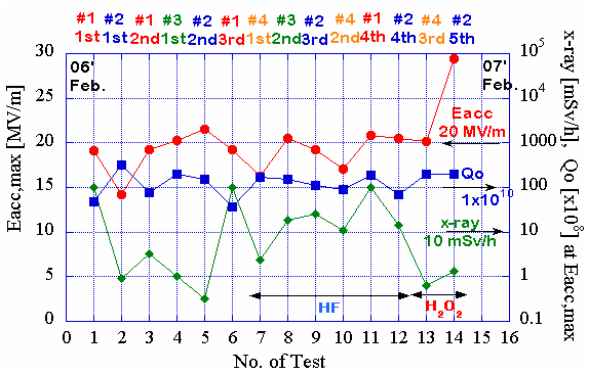

Figure 2: Summary of 14 vertical tests on four cavities; (Eacc,max, Qo value and x-ray level at the Eacc,max).

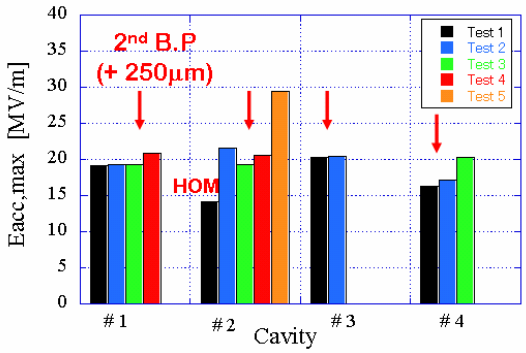

Figure 3: The obtained Eacc,max in each cavity.

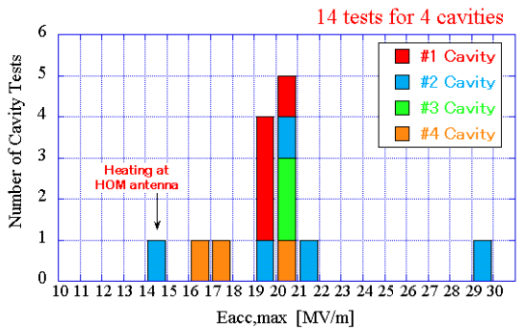

Figure 4: Distribution of the obtained Eacc,max.

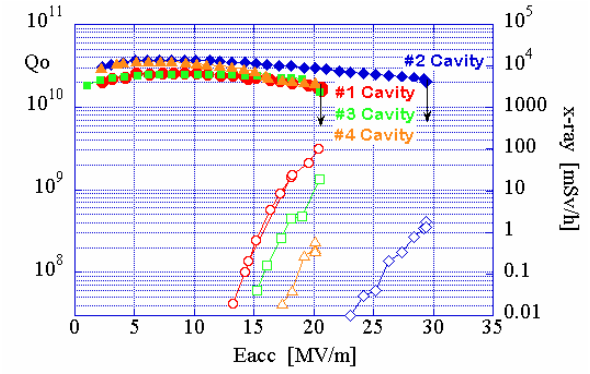

Figure 5: Qo vs. Eacc curves and x-ray radiation level in the final performance on four 9-cell cavities.

Passband-Mode Measurements

After the π-mode measurement, the passband-mode measurements were successively carried out in order to determine the achievable Eacc in the individual cell. Fixed temperature sensors (totally about 40 carbon resisters) were attached at the equator of each cell in every 90 degrees, [8]. Temperature rises in the heating cell during quench events were clearly detected by these sensors. Figure 6 shows one example of the result of the passband-mode measurement in the #2 cavity. In the 4th test (after 2nd barrel polishing), quench induced by impact electrons due to field emission was observed at the #2 cell. In the 5th test (additional surface preparation with EP 20μm and H_2O_2 rinse), the steep Qo drop due to field emission was eliminated, and the x-ray radiation level was shifted to much higher fields. Finally, the Eacc,max was limited at

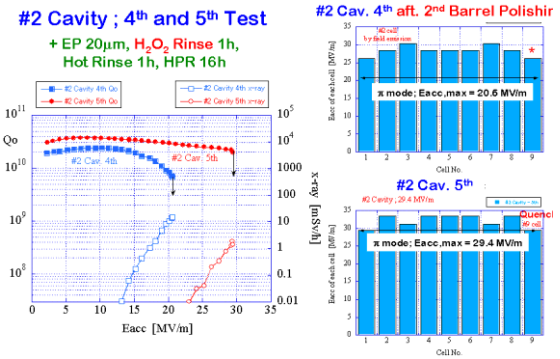

Figure 6: Result of the passband-mode measurement in the #2 cavity, (4th and 5th test).

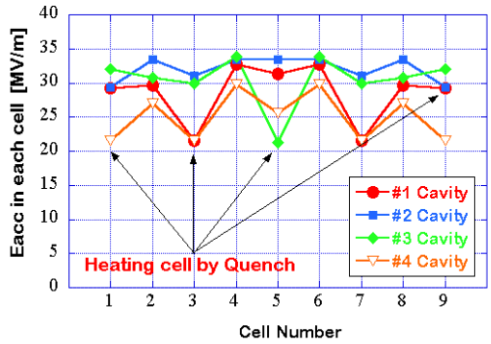

Figure 7: Achievable Eacc in each cell for four cavities.

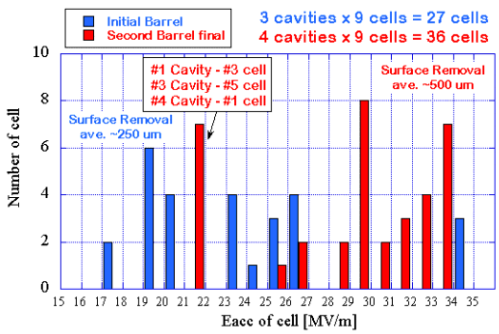

Figure 8: Distribution of the achievable Eacc in each cell before and after the 2nd barrel polishing.

the field close to 30 MV/m with a Qo value of $2x10^{10}$, and the heating cell by quench was in the #9 cell.

The achievable Eacc in the individual cell and the cell limiting the Eacc,max by quench was shown in Fig. 7. The heating cell by quench at the Eacc,max located at random in four cavities. Comparison of the achievable Eacc in each cell between before/after the 2nd barrel polishing is shown in Fig. 8. The distribution of the Eacc has clearly shifted to the higher fields after the 2nd barrel polishing, but only one cell among nine cells still stays around 20 MV/m in three cavities. Therefore, elimination of these cells with a poor performance is necessary to achieve higher gradient in the 9-cell cavities, since the nine-cell performance is determined by only one cell with the lowest Eacc. Therefore, it is considered that further strict quality control is needed both in the cavity fabrication and in the surface preparation. For the next step, improvement of the welding procedure and the clean environment at a company, and construction of the new infrastructure for surface treatments and assembly at KEK are indispensable to achieve reproducibly higher cavity performance.

PECULIAR OBSERVATIONS

Excitation of Another Passband Mode

A strange phenomenon, which Qo value goes up with higher Eacc as shown in Fig. 9, was observed in all cavities after the 2nd barrel polishing. Transition from normal to abnormal state was observed very slowly, (10~60 seconds). In this period, the monitored reflected and transmitted rf power have gradually increased, in spite of the constant incident rf power. In the normal state, the Eacc,max was limited by quench at 21 MV/m, which

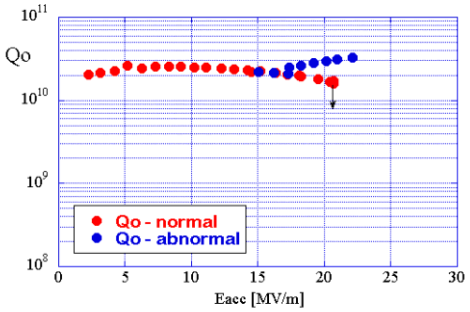

Figure 9: Strange behaviour of Qo values due to the excitation of the 8π/9 passband mode inside the cavity.

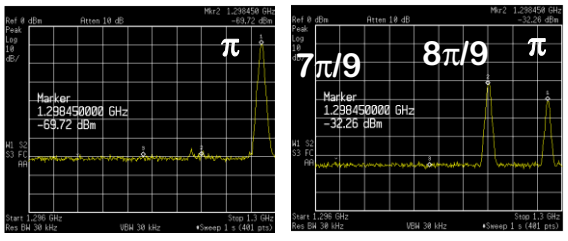

Figure 10: Frequency spectrum of Pin (Left) and Pref (Right) during excitation of another passband mode.

decay time is about 1 msec. In the abnormal state, however, the Eacc,max was finally limited by uncontrollable PLL (phase-lock loop). Occurrence of this phenomenon shifted to higher Eacc by changing the coupling of an input coupler to over-coupling. The frequency spectrum in each monitored rf power was checked as seen in Fig. 10, so that excitation of the 8π/9 mode was observed in the reflected (Pref) and transmitted power, although the incident power (Pin) was only fundamental π mode. Similar phenomenon was also observed in the TESLA cavities at DESY, however, the excited passband-mode was not the 8π/9 mode but the 7π/9 mode, [9]. One potential explanation is that field emission current might be possible to excite a parasitic mode.

Heating at the HOM Pickup Antenna

Slow quench, which the decay time of Eacc was about 10 seconds, was occurred at ~14 MV/m. The drop of the Qo value was observed, and the degraded Qo value was still kept even at low fields. It took very long time more than 30 minutes to recover the Qo value. This cycle was reproducibly repeated, as shown in Fig. 11. It was thought that transition from a superconducting state to a normal conducting state seemed to be occurring at an isolated location thermally. It was found that this phenomenon was caused by heating at a tip of the HOM pickup antenna made of niobium. This phenomenon was eliminated by shortening the antenna length in the 2nd test, as shown in Fig. 12, [10].

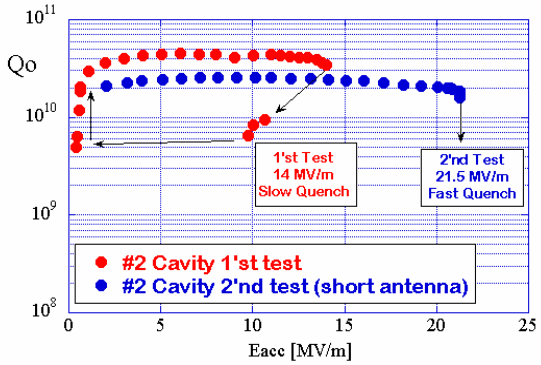

Figure 11: Degradation of Qo values due to heating at the HOM pickup antenna.

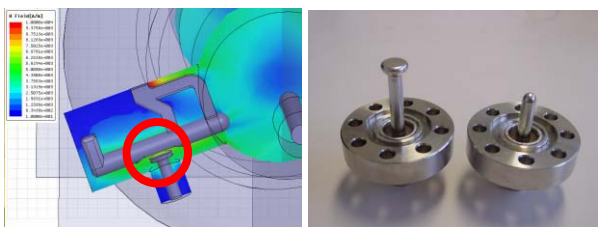

Figure 12: Calculated magnetic field distribution (Left) and the initial antenna shape and a short antenna (Right).

Multipacting at HOM Couplers

Quench events were frequently observed at rather low field levels. Several temperature sensors were attached at the outside near the gap of the HOM couplers, as shown in Fig. 13, (Left). Temperature rises due to multipacting at these locations was clearly observed as seen in Fig. 13 (Right). Processing of this multipacting level has easily finished during a comparatively short time for several minutes. After the processing, quench due to multipacting at the HOM couplers had not reappeared. Therefore, this phenomenon was not a final cause limiting the Eacc,max.

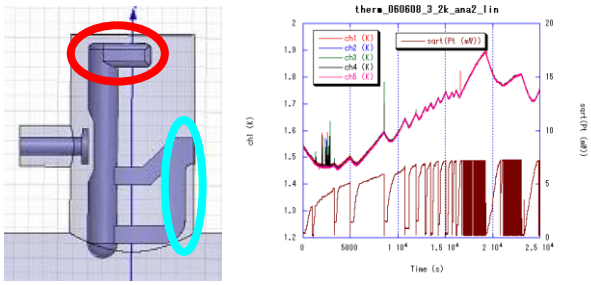

Figure 13: Location of multipacting (Left) and observation of temperature rises by thermometry (Right).

Degradation of Field Flatness due to EP

It is very important to maintain the field flatness after the pre-tuning procedure. Checking the field flatness before the final EP and after the vertical test was always carried out, and change of the field flatness in each cavity

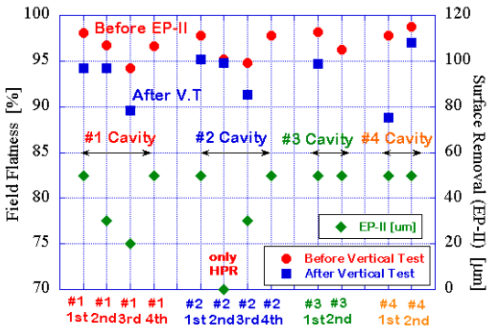

Figure 14: Change of the field flatness before/after vertical tests (V.T) and the surface removal by EP.

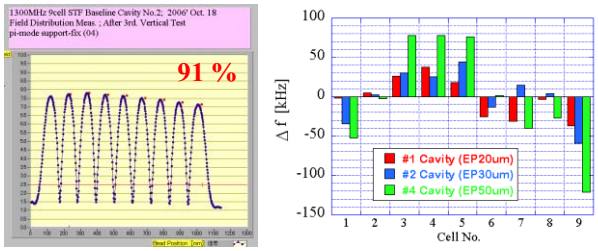

Figure 15: Field distribution after a vertical test (Left) and frequency shift (Δf) in each cell before/after V.T (Right).

test is summarised in Fig. 14. Degradation of the field flatness after the vertical test was less than about 4%, except one case. A measured field distribution after a vertical test is shown in Fig. 15 (Left), and this pattern was very similar in every cavity; *i.e.*, the field in both end-cells is weaker than that in the other center-cells. The frequency shift (deviation from an ideal frequency) in each cell on the different surface removal by EP is shown in Fig. 15 (Right). This result shows that the amount of surface removal by EP seems to be not uniform in each cell. Moreover, measurements of the temperature outside of the cells and the acid flow rate inside the cell during EP process showed a very similar distribution as the frequency shift. Therefore, improvement of the acid flow rate in each cell and the correct temperature control for EP is necessary to maintain an acceptable field flatness.

ASSEMBLY OF CRYOMODULE

Dressing of the He Jacket

After the cavity performance was qualified in the vertical tests, the four cavities were transported to a company. The four cavities were covered with a titanium jacket for filling liquid He at 2 K, as shown in Fig. 16.

Figure 16: Before and after TIG welding of a He jacket. A magnetic shield (centre in left) was inserted in a He jacket.

Installation in the Cryomodule

One cavity for the STF Phase-0.5 was assembled with an input coupler and a gate-valve in a new clean room (class-10), as shown Fig. 17. The cavity equipped with a tuner system was installed in one of the 6m-cryomodules. The first cool-down of the cryomodule in the tunnel, as shown in Fig. 18, had been started in October, 2007. High power rf test of the cavity is scheduled in November. String assembly of four cavities for the STF Phase-1 will be carried out in December for the next step.

Figure 17: Installation of an input coupler (Left) and an assembled cavity mounted on 2 K gas return pipe (Right).

Figure 18: STF cryomodule connected with a cold valve box for the first cool-down test in the tunnel.

ACKNOWLEDGMENTS

The authors are indebted to K. Sennyu and H. Hara (MHI, Mitsubishi Heavy Industries) for the fabrication of the 9-cell cavities. Special thanks are given to T. Suzuki and S. Fukuda (Nomura Plating Co., Ltd.) for the surface preparation of the 9-cell cavities.

REFERENCES

[1] H. Hayano, "Superconducting RF Test Facility (STF) in KEK", SRF2005, Cornell Univ., Ithaca, NY, USA (2005) p409-411.

[2] S. Noguchi, et al., "STF Baseline Cavities and RF Components", SRF2005, Cornell Univ., Ithaca, USA, (2005), http://www.lns.cornell.edu/public/SRF2005/. Also, presentation for the ILC seminar at KEK, (May 11th, 2007), http://lcdev.kek.jp/LocalMeetings/.

[3] E. Kako, et al., "Construction of the STF Baseline Cavity System for STF at KEK", PAC07, Albuquerque, NM, USA, (2007) p2107-2109.

[4] E. Kako, et al., "High Power Input Couplers for the STF Baseline Cavity System at KEK", SRF2007, Peking Univ., Beijing, China, (2007) TUP60 in this proceedings.

[5] K. Watanabe, et al., "Higher Order Mode Study of Superconducting Cavity for ILC Baseline", EPAC06, Edinburgh, Scotland, (2006) p747-749.

[6] S. Noguchi, "Review of New Tuner Design", SRF2007, Peking Univ., Beijing, China, (2007) WE303 in this proceedings.

[7] K. Sennyu, et al., "Design and Fabrication of Superconducting Cavities for Industrialization", SRF2007, Peking Univ., Beijing, China, (2007) WEP48 in this proceedings.

[8] Y. Yamamoto, et al., "Cavity Diagnostic System for the Vertical Test of the Baseline SC Cavity in KEK-STF", SRF2007, Peking Univ., Beijing, China, (2007) WEP13 in this proceedings.

[9] D. Proch, private communication.

[10] K. Watanabe, et al., "New HOM Coupler Design for ERL injector at KEK", SRF2007, Peking Univ., Beijing, China, (2007) WEP30 in this proceedings.